Electronic Supplementary Material (ESI) for ChemComm.
This journal is © The Royal Society of Chemistry 2023

Supplementary Information

A heteroleptic fused bi-cuboctahedral $Cu_{21}S_2$ cluster

Rhone P. Brocha Silalahi,[a] Tzu-Hao Chiu,[a] Hao Liang,[b] Samia Kahlal,[b] Jean-Yves Saillard,[b]* and C. W. Liu [a]*

[a]Department of Chemistry, National Dong Hwa University No. 1, Sec. 2, Da Hsueh Rd. Shoufeng, Hualien 974301 (Taiwan R.O.C.) E-mail:chenwei@gms.ndhu.edu.tw

[b]Univ Rennes, CNRS, ISCR-UMR 6226, F-35000 Rennes (France)

Experimental Section

Materials and Measurement

All the reactions were carried out under an N_2 atmosphere using the standard Schlenk technique. The solvents used in this work were distilled before use, following standard protocols. All chemicals were purchased from different commercial sources available and used as received. $[Cu(CH_3CN)_4](PF_6)$,[1] $[K\{S_2CN^nBu_2\}]$,[2] and $[Cu_{15}H_2\{S_2CN^nBu_2\}_6(C_2Ph)_6]$[3] were prepared by following the procedures reported in the literature. NMR spectra were recorded on a Bruker Advance DPX300 FT-NMR spectrometer that operates at 400 MHz while recording ^1H, 121.5 MHz for $^{31}P\{^1H\}$, and 100.61 MHz for ^{13}C. Used residual solvent proton references: δ, 7.26 ($CDCl_3$) and 2.10 (d_6-acetone). The $^{31}P\{^1H\}$ NMR spectra were referenced to external 85% H_3PO_4 at δ = 0.00 ppm. The chemical shift (δ) is reported in ppm. ESI-mass spectra were recorded on a Fison Quattro Bio-Q (Fisons Instruments, V.G. Biotech, U. K.). UV–Visible absorption spectra were measured on a Perkin Elmer Lambda 750 spectrophotometer using quartz cells with a path length of 1 cm.

Synthesis of $[Cu_{21}S_2\{S_2CN^nBu_2\}_9(C_2Ph)_6](PF_6)_2$

Synthesis of $[Cu_{21}S_2\{S_2CN^nBu_2\}_9(C_2Ph)_6](PF_6)_2$ can be prepared by following three procedures:

By using $[Cu_{15}H_2\{S_2CN^nBu_2\}_6(C_2Ph)_6](PF_6)$ as template cluster

In a flame-dried Schlenk tube **[**$Cu_{15}H_2\{S_2CN^nBu_2\}_6(C_2Ph)_6](PF_6)$ (0.05 g; 0.017 mmol) was added to a flask along with 10 mL acetone solvent; then trifluoroacetic acid (0.002 mL; 0.034 mmol) was added under vigorous stirring. The reaction was aged 10 minutes under an N_2 atmosphere at room temperature. The solvent was evaporated under a vacuum, and the residue was extracted with water and ethyl acetate (3×15 mL). The ethyl acetate layer was collected and dried. The orange-red residue was washed with methanol to remove the impurities and dissolved in acetone. The filtrate was evaporated to dryness under vacuum to give orange-red powder of $\mathbf{Cu_{21}S_2}$ in 15 % yields.

By using $[Cu_{12}S\{S_2CN^nBu_2\}_6(C_2Ph)_4]$ as template cluster

In a flame-dried Schlenk tube $[Cu_{12}S\{S_2CN^nBu_2\}_6(C_2Ph)_4]$ (0.05 g; 0.0206 mmol), and NBu_4PF_6 (0.008 g; 0.021 mmol) was added to a flask along with 10 mL CH_3Cl solvent; then trifluoroacetic acid (0.002 mL; 0.041 mmol) was added under vigorous stirring. The reaction was aged 10 minutes under an N_2 atmosphere at room temperature. The solvent was evaporated

under a vacuum, and the residue was extracted in water and ethyl acetate (3×15 mL). The ethyl acetate layer was collected and dried. The residue was washed with methanol to get rid of the impurities. The orange-red was collected in acetone and evaporated to dryness under a vacuum to give an orange-red powder of **$Cu_{21}S_2$** in 20 % yields based on Cu.

By using the one-pot synthesis method

In a flame-dried schlenk tube, phenylacetylene (0.08 mL; 0.66 mmol) and trimethylamine (0.08 mL; 0.55 mmol) were suspended in THF-CH_3CN (*v:v*=5:5) mixed solvent (30 mL) at room temperature. After stirring for 5 minutes, the resulting mixture was heated to 50°C followed by the addition [K{S2CN^{n}Bu$_2$}] ligand (0.09 g; 0.37 mmol), followed by $Na_2S_2O_3$ (0.01 g; 0.06 mmol), which already dissolved in water. The mixture kept stirring under the N_2 atmosphere. $[Cu(CH_3CN)_4](PF_6)$ (0.26 g; 0.69 mmol) was added and kept under continuous stirring for 4 hours. The reaction mixture was then filtered to remove any solids, and the filtrate was evaporated to dryness under a vacuum to give orange-red powder. The residue was washed with methanol. The orange-red residue was extracted in acetone and dried under vacuum to get an orange-red precipitate of **$Cu_{21}S_2$** in 23 % yields based on Cu.

$[Cu_{21}S_2\{S_2CN^nBu_2\}_9(C_2Ph)_6](PF_6)_2$ ($Cu_{21}S_2$): ESI-MS: *m/z* at 1921.86 Da (calc. *m/z* at 1921.74 Da) for $[Cu_{21}S_2\{S_2CN^nBu_2\}_9(C_2Ph)_6]^{2+}$. ^{1}H NMR (400 MHz, d_6-acetone): 7.60-7.42 (30H, -C_6H_5), 4.23-4.02 (36H, CH_2), 1.89-1.72 (36H, CH_2), 1.44-1.29 (36H, CH_2), 0.98-0.84 (54H, CH_3) ppm. ^{31}P{^{1}H} NMR (121.5 MHz, d_6-acetone): -143.11 $(PF_6)^-$ ppm. ^{13}C NMR (100.61 MHz, $CDCl_3$): 201.33, 131.99, 128.03, 123.81, 122.86, 80.05, 77.27, 57.54, 28.93, 19.93, and 13.62.

Synthesis of $[Cu_{12}S\{S_2CN^nBu_2\}_6(C_2Ph)_4]$

In a flame-dried schlenk tube, phenylacetylene (0.08 mL; 0.66 mmol) and trimethylamine (0.08 mL; 0.55 mmol) were suspended in THF-CH3CN (v:v=5:5) mixed solvent (30 mL) at room temperature. After stirring for 5 minutes, the resulting mixture was cooled down to 0°C followed by the addition of [K{$S_2CN^nBu_2$}] ligand (0.06 g; 0.26 mmol), followed by the addition of $Na_2S_2O_3$ (0.005 g; 0.03 mmol) which already dissolved in water. The mixture kept stirring under the N_2 atmosphere. $[Cu(CH_3CN)_4](PF_6)$ (0.20 g; 0.57 mmol) was added and kept under continuous stirring for 4 hours. The reaction mixture was filtered to remove any solids, and the filtrate was evaporated to dryness under a vacuum to give yellow powder and washed

with methanol to remove the impurities. The yellow residue was extracted in acetone and dried under vacuum to get a yellow precipitate of **$Cu_{12}S$** in 28 % yields based on Cu.

[$Cu_{12}S\{S_2CN^nBu_2\}_6\{C_2Ph\}_4$] ($Cu_{12}S$): ESI-MS: *m/z* at 2426.35 Da (calc. *m/z* 2424.81 Da) for [$Cu_{12}S\{S_2CN^nBu_2\}_6\{C_2Ph\}_4$+$H^+$]$^+$. ^{1}H NMR (400 MHz, d_6-acetone): 7.39-7.53 (20H, -C_6H_5), 4.02 (24H, CH_2), 1.73 (24H, CH_2), 1.32 (24H, CH_2), 0.87 (36H, CH_3) ppm.

Single-Crystal X-ray Crystallography

The single crystals of **$Cu_{21}S_2$** were mounted on the tip of glass fiber coated with paratone oil, then frozen. Data were collected on a Bruker APEX II CCD diffractometer using graphite monochromated Mo Kα radiation (λ = 0.71073 Å) at 100K. Absorption corrections for the area detector were performed with SADABS,[4] and the integration of the raw data frame was performed with SAINT.[5] The structure was solved by direct methods and refined by least-squares against F^2 using the SHELXL-2018/3 package,[6,7] incorporated in SHELXTL/PC V6.14.[8] CCDC no. 2269528 contains the supplementary crystallographic data in this article. The data can be obtained free from The Cambridge Crystallographic Data Centre via www. ccdc.cam.ac.uk/data_request/cif. In the x-ray structure, all F atoms on one of the $[PF_6]^-$ ions disorder in two positions with 50% occupancy (F1 and F2) (Figure S17); the second $[PF_6]^-$ anion is located in the unique symmetric position. This increases the difficulty in accurately determining four F atoms on the $[PF_6]^-$ belt. We have tried our best to distribute the four F atoms evenly among the six symmetric positions and the model is shown in Figure S18.

We have provided a response of the check cif alerts.

start Validation Reply Form

_vrf_PLAT232_$Cu_{21}S_2$

PROBLEM: Hirshfeld Test Diff (M-X) Cu1 --S4 . 20.6 s.u.

Hirshfeld Test Diff (M-X) Cu2 --S4 . 28.7 s.u.

RESPONSE: This alert might be caused by the S atom on a special position.

end Validation Reply Form

Computational details

DFT calculations were carried out using the Gaussian (R) 16 program.[9] The split valence polarization (def2-SVP) basis set[10] and the BP86[11,12] exchange-correlation functional were used, which provides reliable ground-state results for metal NCs at a reasonable

computational cost. All the optimized structures were confirmed as true minima on their potential energy surface by analytical vibration frequency calculations. Natural atomic orbital (NAO) populations and Wiberg bond indices were computed with the natural bond orbital NBO 6.0 program[13-15] implemented in the Gaussian (R) 16 package. The UV-visible transitions were calculated by means of TD-DFT calculations with the same basis set but with the hybrid CAM-B3LYP functional,[16] which provides more reliable results with respect to optical properties (although at a higher computational cost) than the BP86 functional. The UV-visible spectra were simulated from the computed TD-DFT transitions and their oscillator strengths using the SWizard program,[17] each transition being associated with a Gaussian function of half-height width equal to 3000 cm^{-1}.

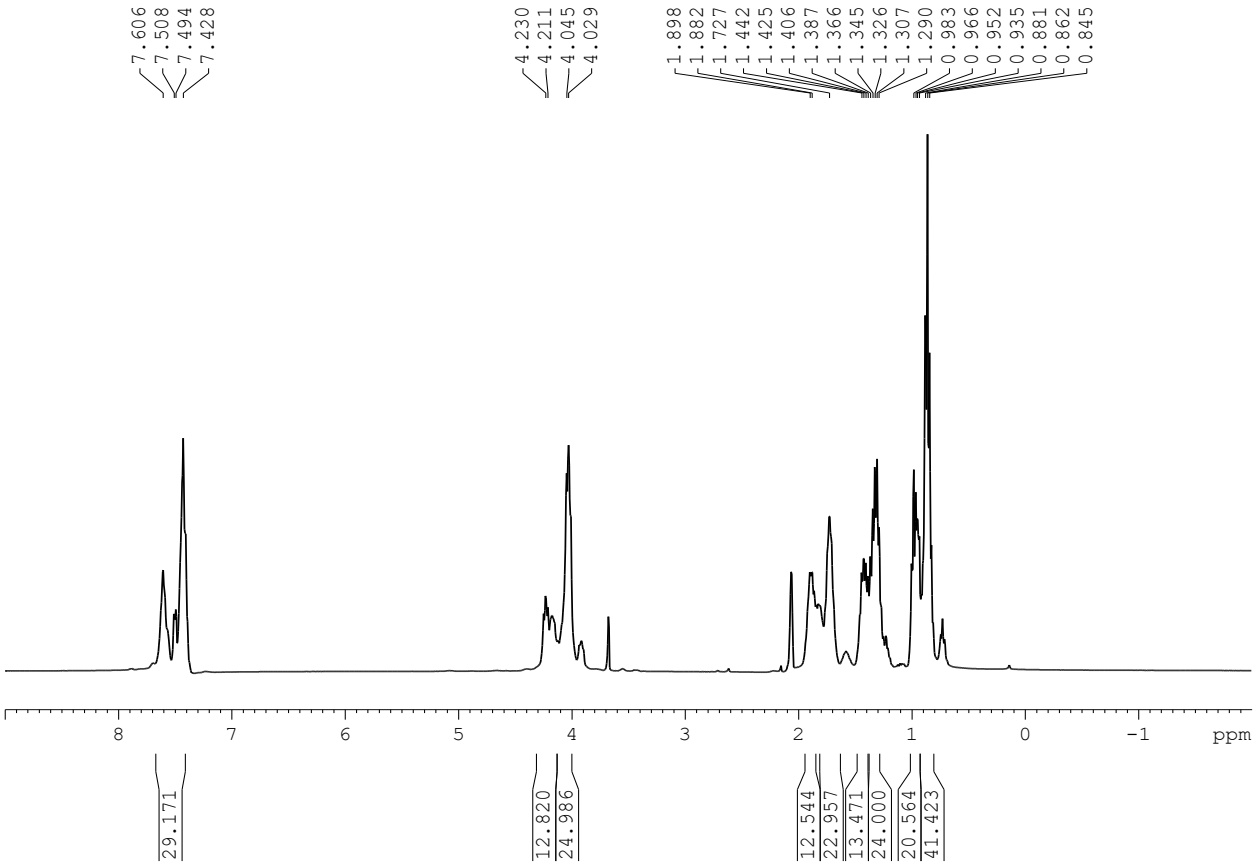

Figure S1. ^{1}H NMR spectrum of $\mathbf{Cu_{21}S_2}$ in d_6-acetone.

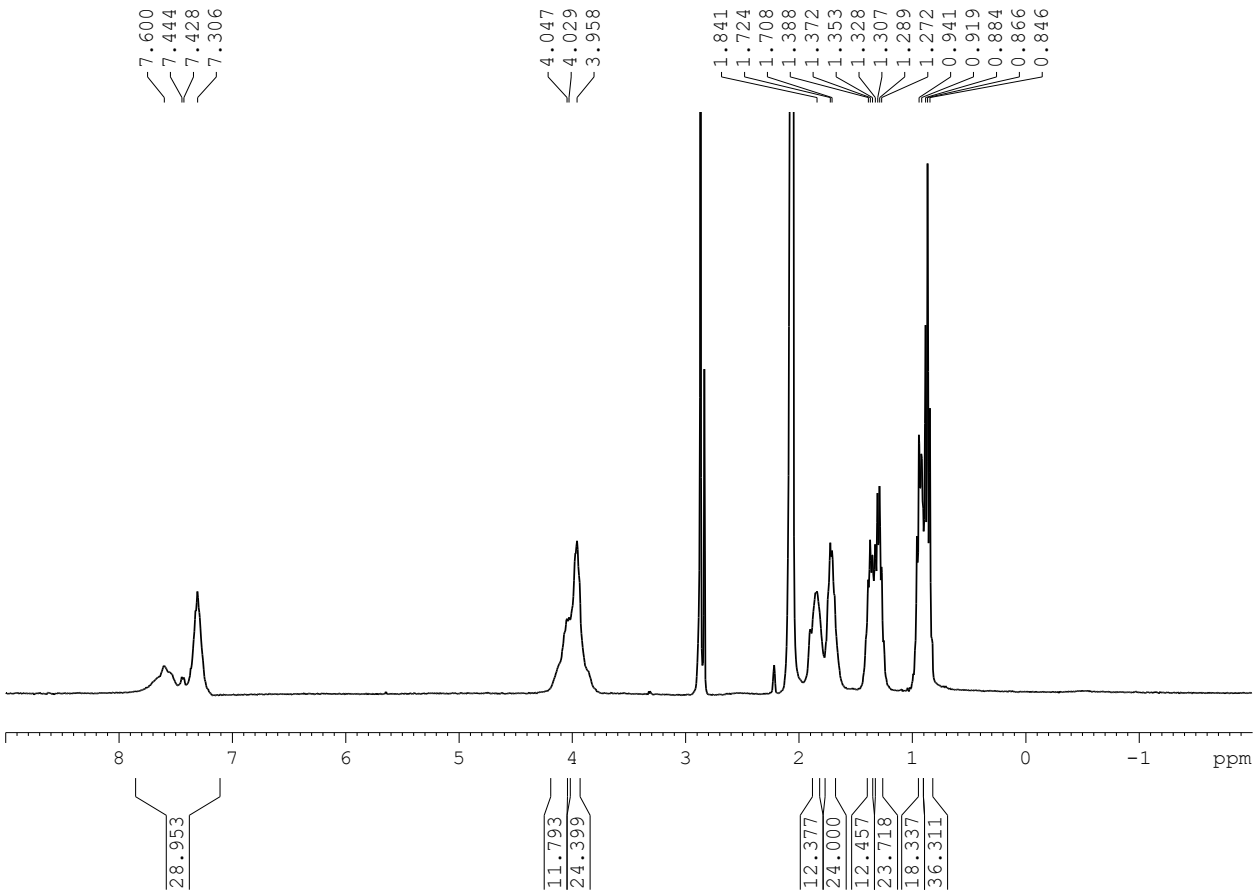

Figure S2. ^{1}H NMR spectrum of $\mathbf{Cu_{21}S_2}$ crystal in d_6-acetone.

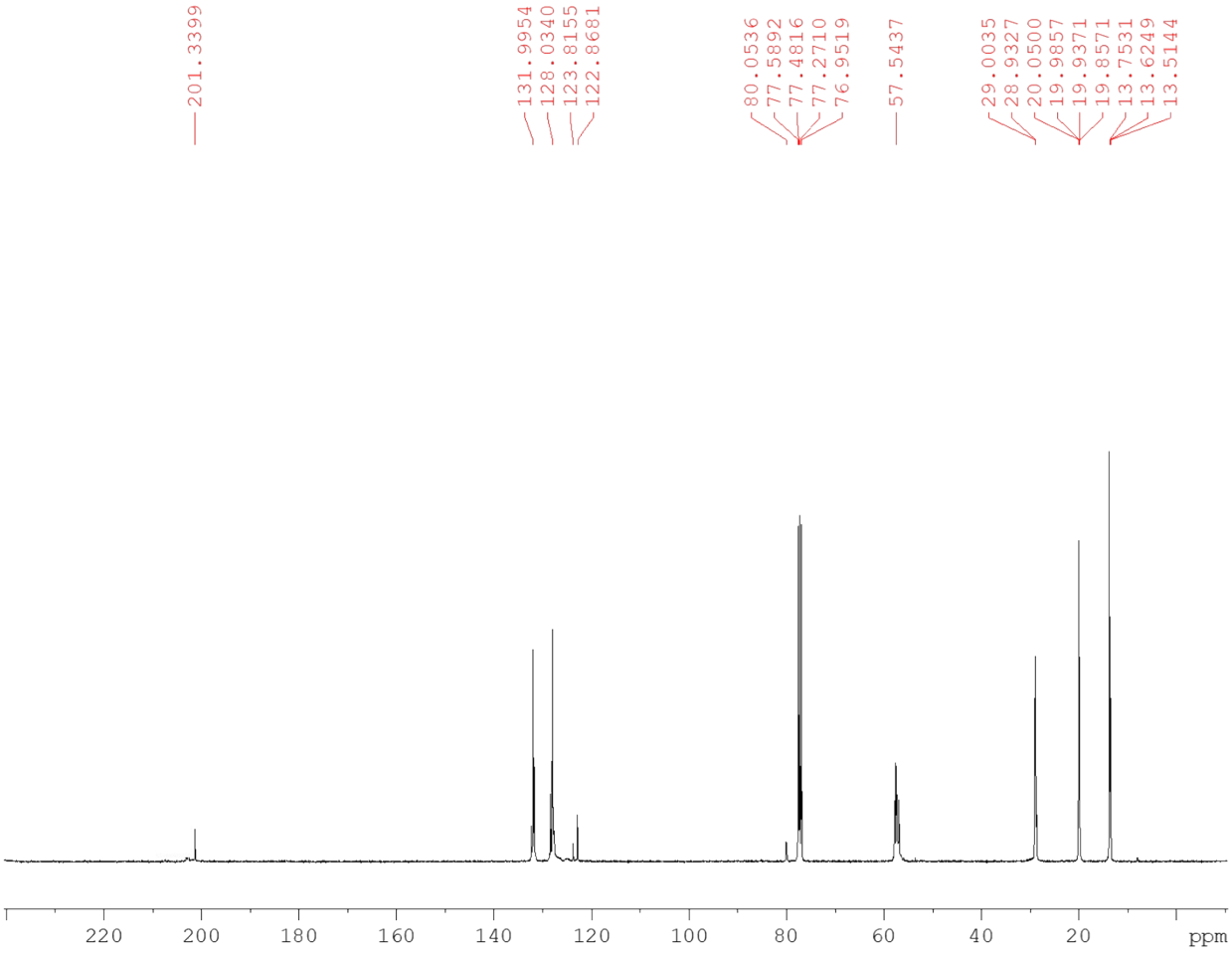

Figure S3. ^{13}C NMR spectrum of $\mathbf{Cu_{21}S_2}$ in $CDCl_3$.

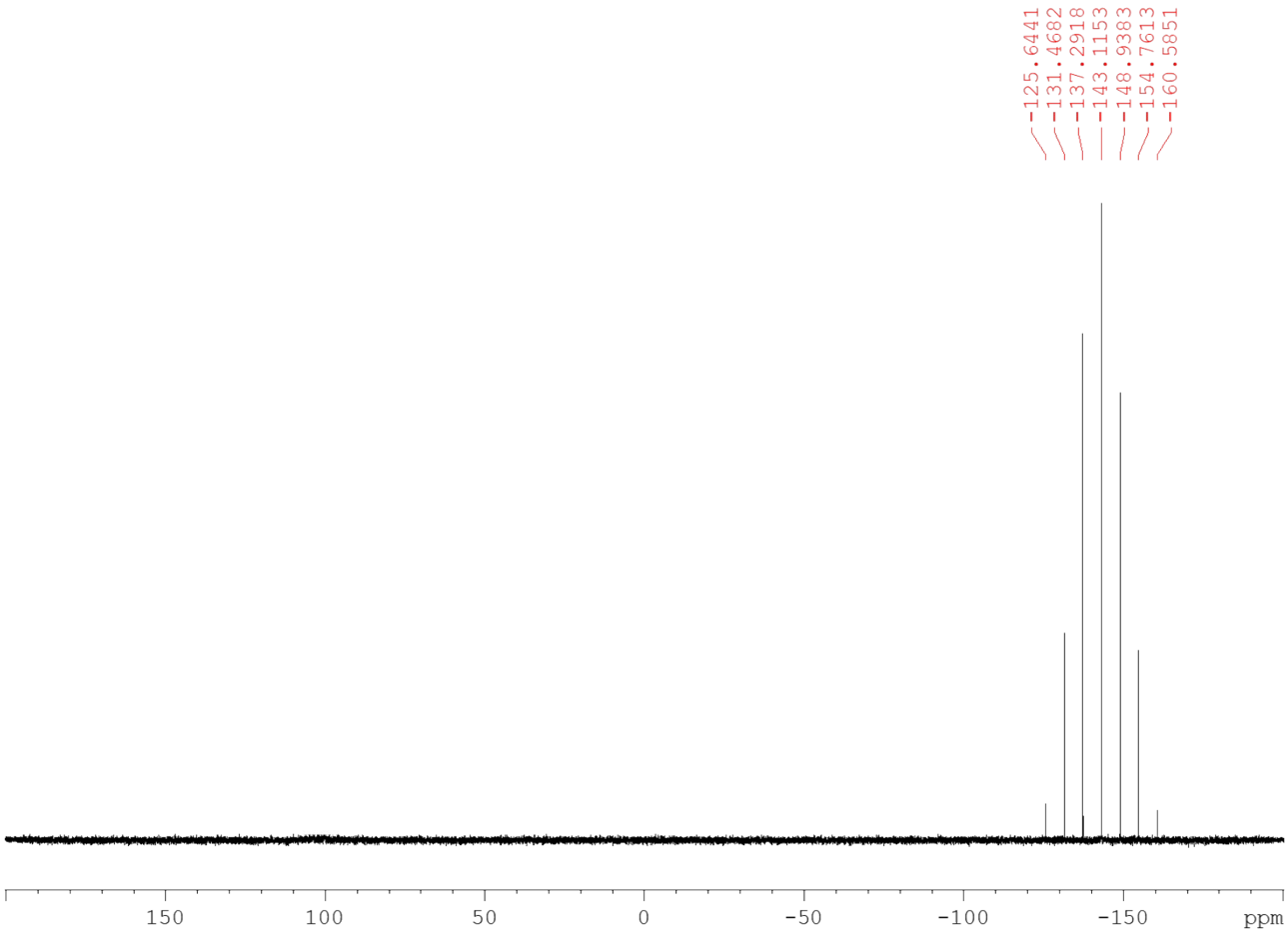

Figure S4. $^{31}P\{^{1}H\}$ NMR spectrum of $\mathbf{Cu_{21}S_2}$ in d_6-acetone.

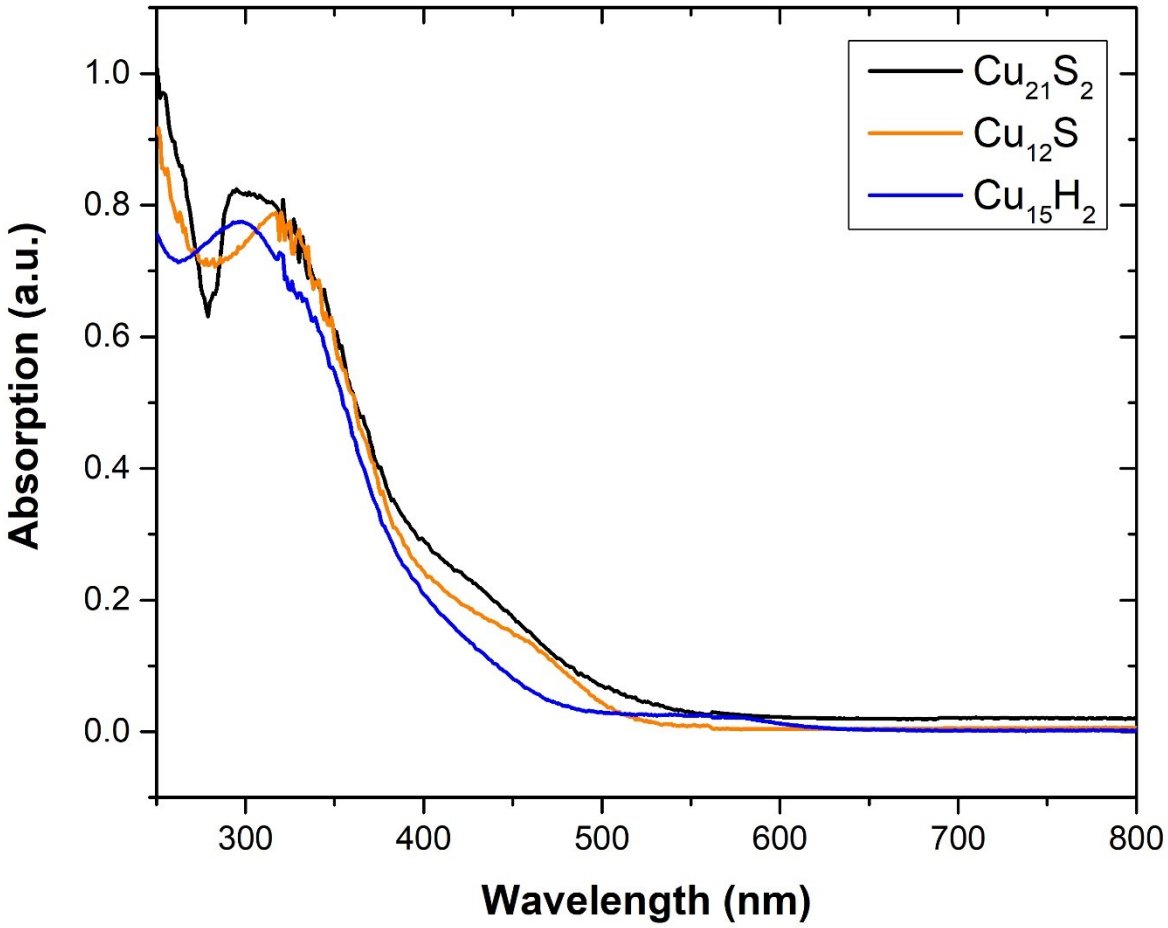

Figure S5. Comparing UV-vis spectra of **$Cu_{21}S_2$**, **$Cu_{12}S$**, and **$Cu_{15}H_2$**.

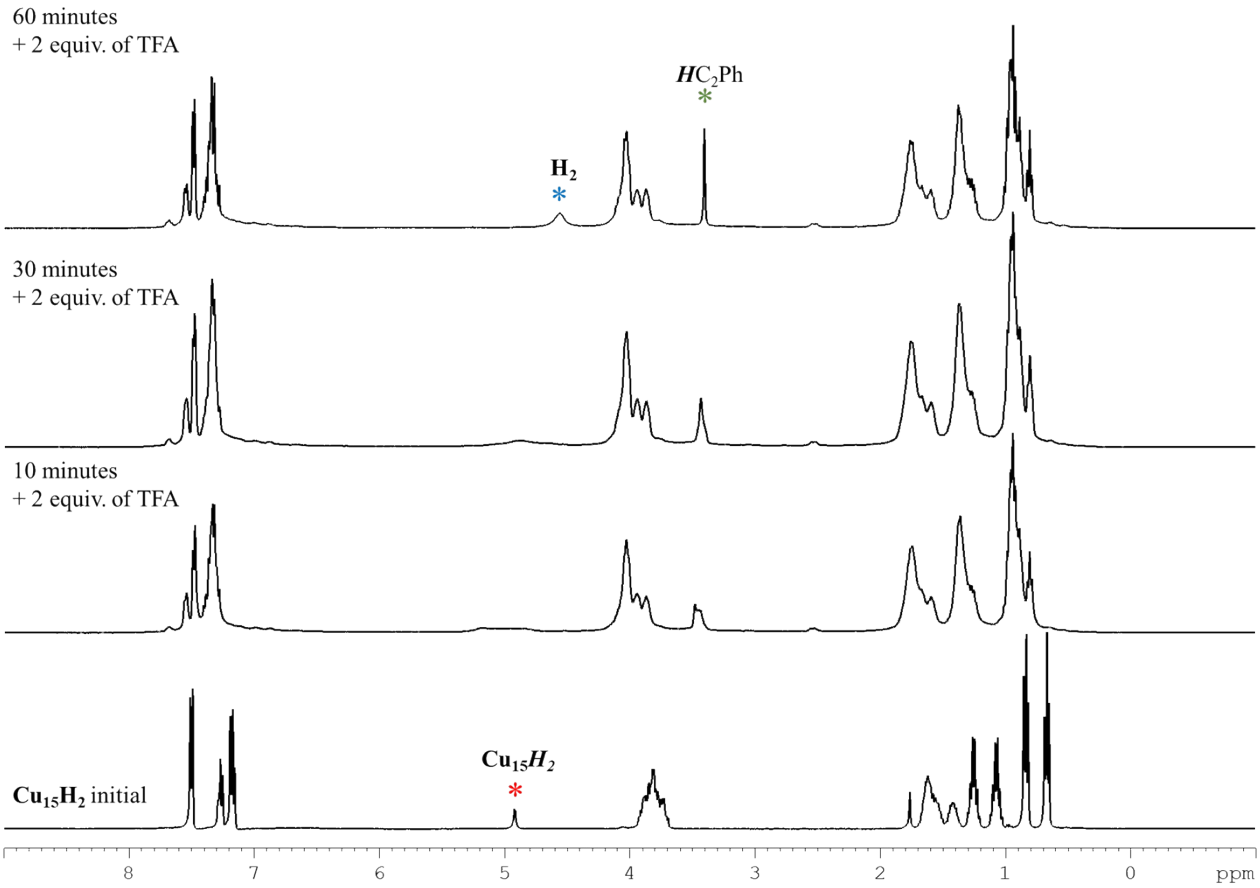

Figure S6. The time-dependent ^{1}H NMR spectra of reaction $\mathbf{Cu_{15}H_2}$ and two equiv. of TFA in $CDCl_3$.

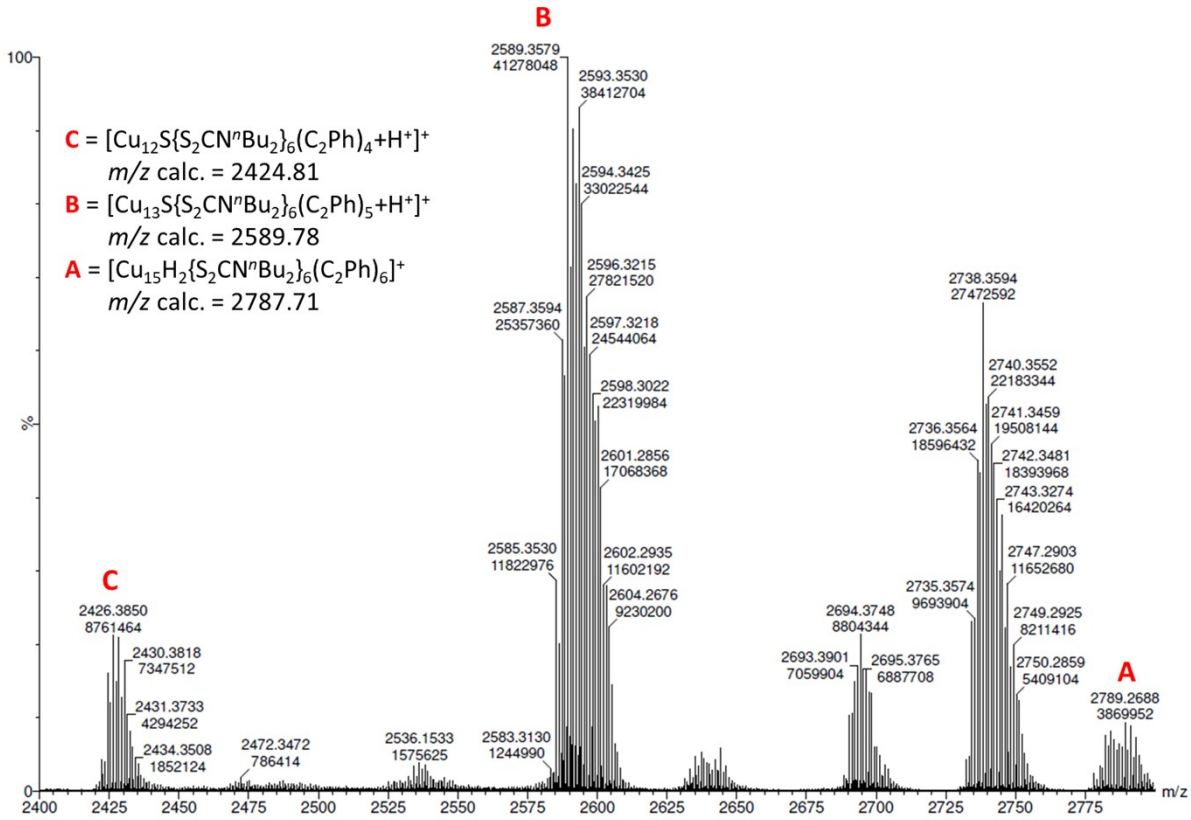

Figure S7. The ESI-MS spectra of reaction $\mathbf{Cu_{15}H_2}$ and two equiv. of TFA.

A. $[Cu_{15}H_2\{S_2CN^nBu_2\}_6(C_2Ph)_6]^+$
m/z exp. = 2789.27
m/z calc. = 2787.71

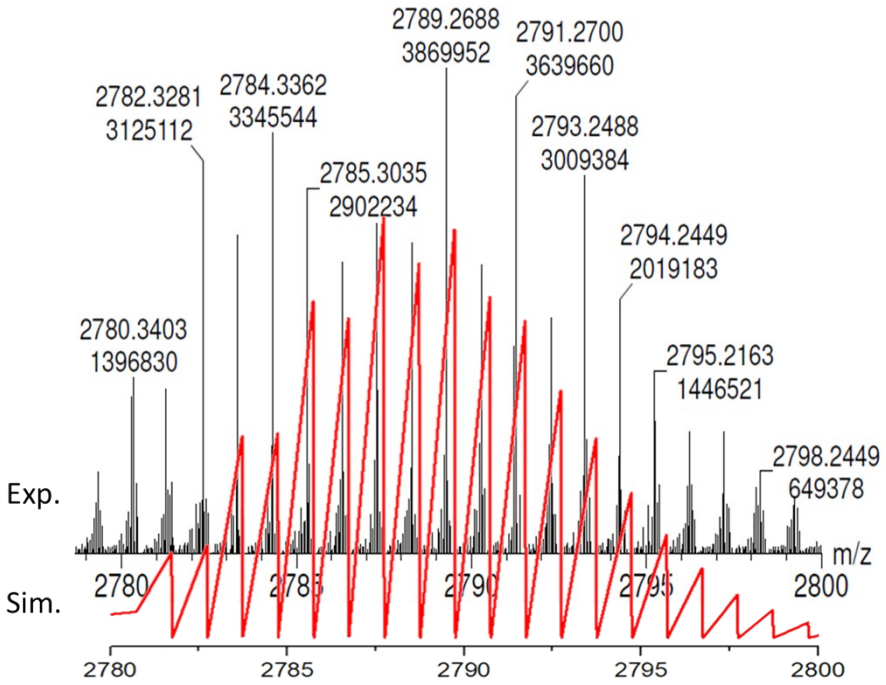

Figure S8. Comparison between experimental (black trace) and simulated (red trace) isotopic patterns of the molecular peaks $[Cu_{15}H_2\{S_2CN^nBu_2\}_6(C_2Ph)_6]^+$.

B. $[Cu_{13}S\{S_2CN^nBu_2\}_6(C_2Ph)_5+H^+]^+$
m/z calc. = 2589.78
m/z exp. = 2589.36

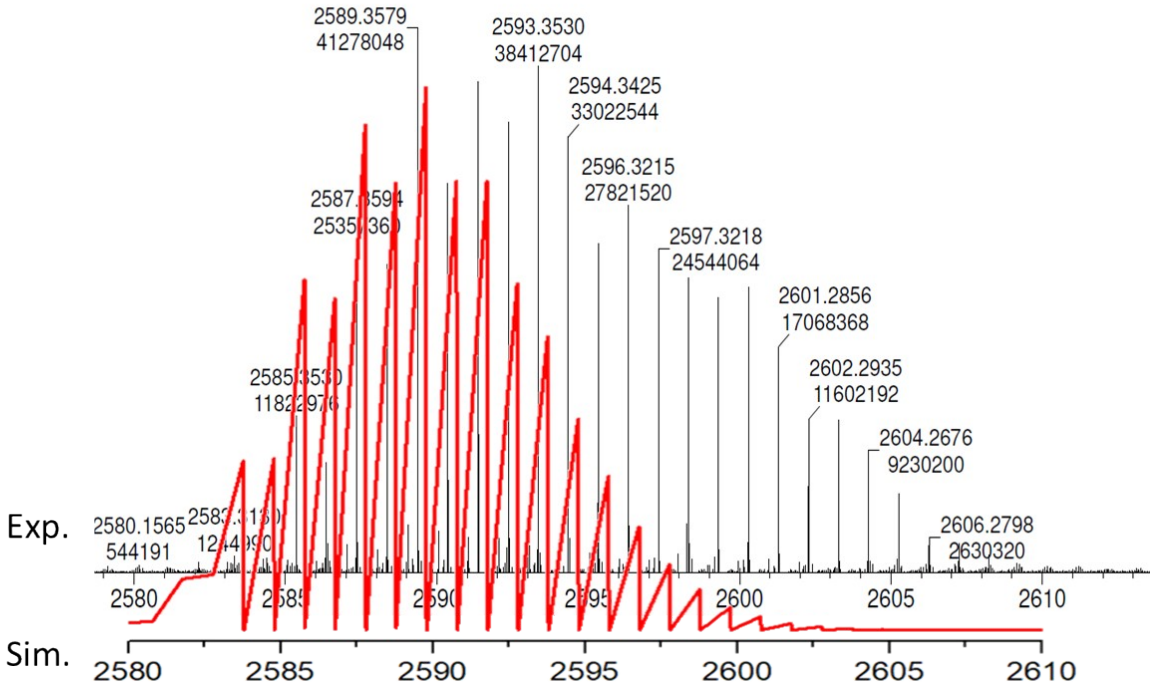

Figure S9. Comparison between experimental (black trace) and simulated (red trace) isotopic patterns of the molecular peaks $[Cu_{13}S\{S_2CN^nBu_2\}_6(C_2Ph)_5+H^+]^+$.

C. $[Cu_{12}S\{S_2CN^nBu_2\}_6(C_2Ph)_4+H^+]^+$
m/z calc. = 2424.81
m/z exp. = 2426.39

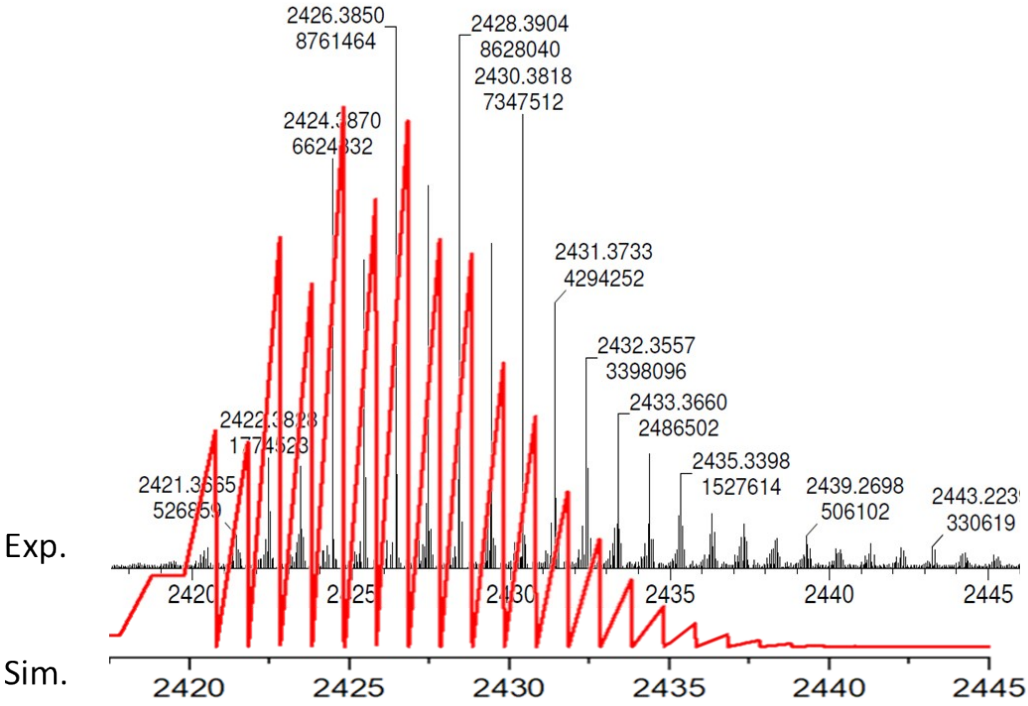

Figure S10. Comparison between experimental (black trace) and simulated (red trace) isotopic patterns of the molecular peaks $[Cu_{12}S\{S_2CN^nBu_2\}_6(C_2Ph)_4+H^+]^+$.

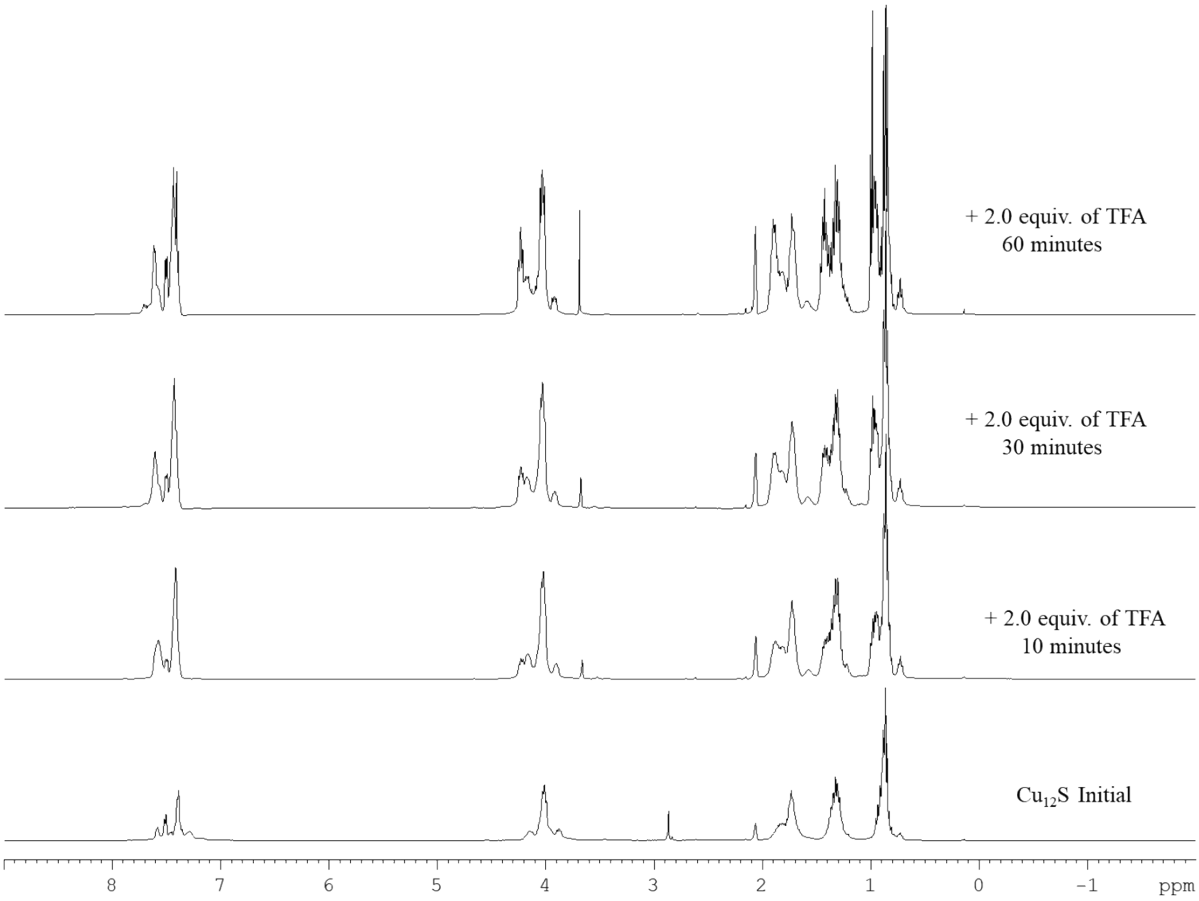

Figure S11. The time-dependent ^{1}H NMR spectra of reaction **$Cu_{12}S$** and two equiv. of TFA in d_6-acetone.

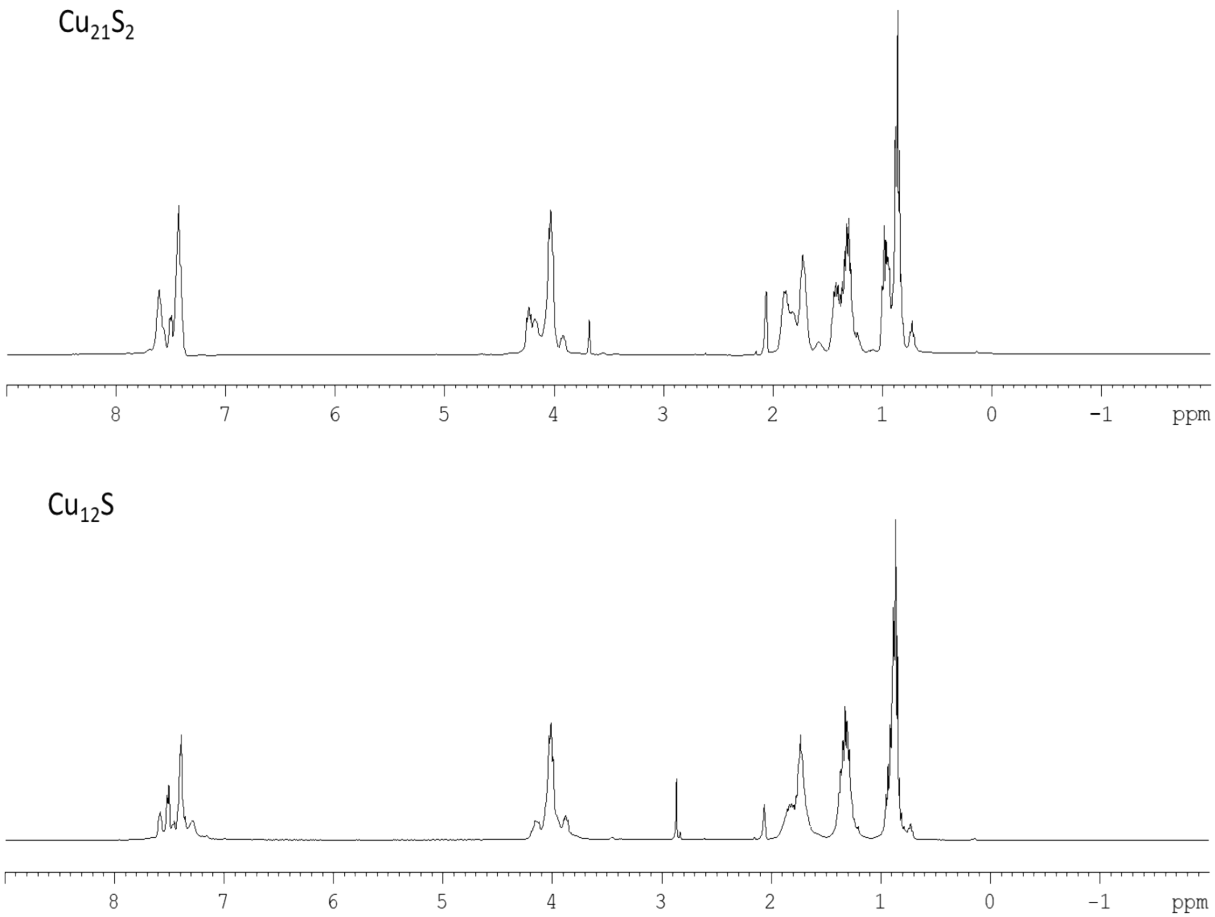

Figure S12. The comparison ^{1}H NMR spectra of **$Cu_{12}S$** and **$Cu_{21}S_2$** in d_6-acetone.

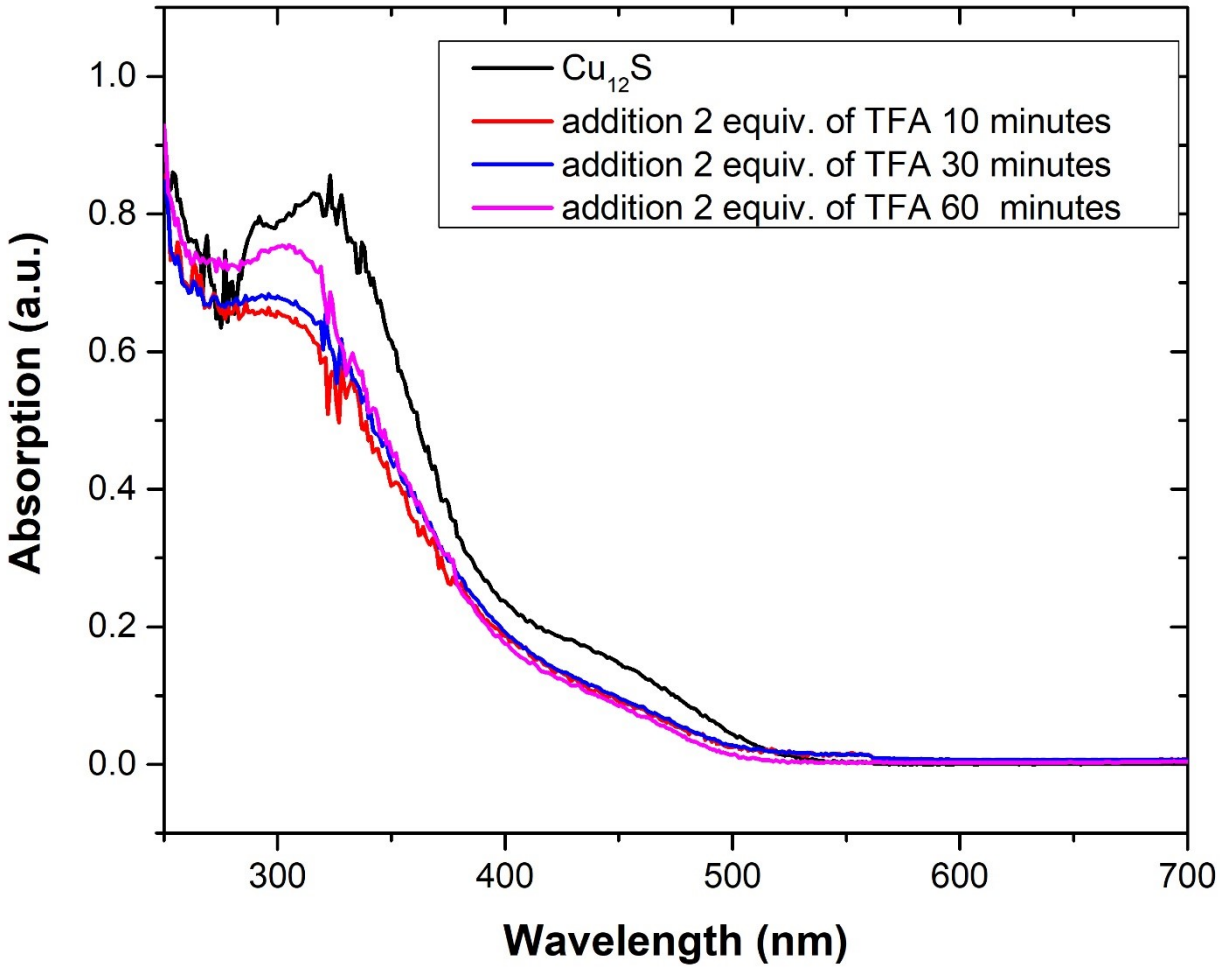

Figure S13. Time-dependent of UV-Visible spectrum degradation **$Cu_{12}S$** into **$Cu_{21}S_2$** after adding two equiv. of TFA in $CHCl_3$.

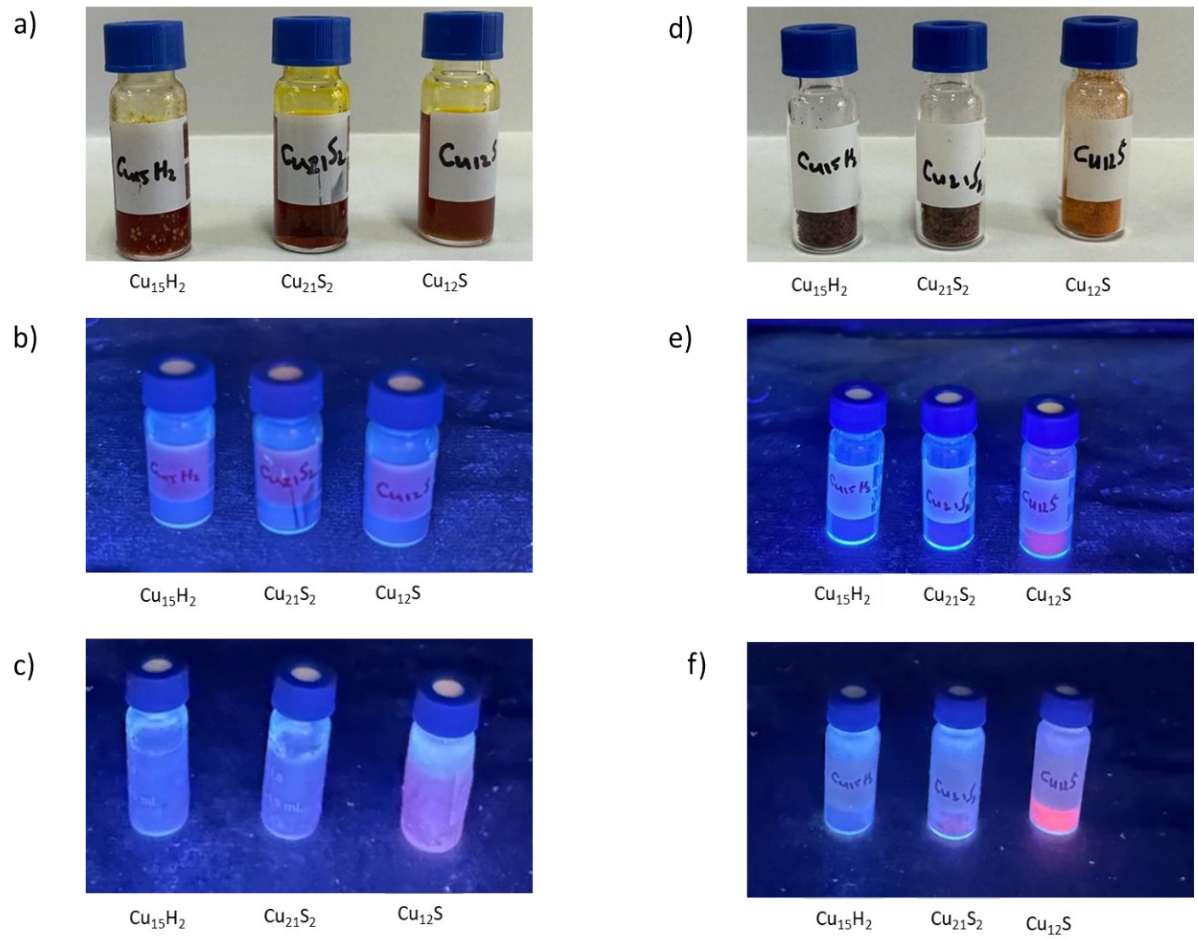

Figure S14. Digital photographs of **$Cu_{15}H_2$**, **$Cu_{21}S_2$**, and **$Cu_{12}S$** solution in a) naked eye in ambient temperature, b) under UV-lamp at room temperature, and c) under UV-lamp in 77 K. **$Cu_{15}H_2$**, **$Cu_{21}S_2$**, and **$Cu_{12}S$** solid state as seen with d) naked eye at ambient temperature, e) under UV-lamp at room temperature, and f) under UV-lamp at 77 K.

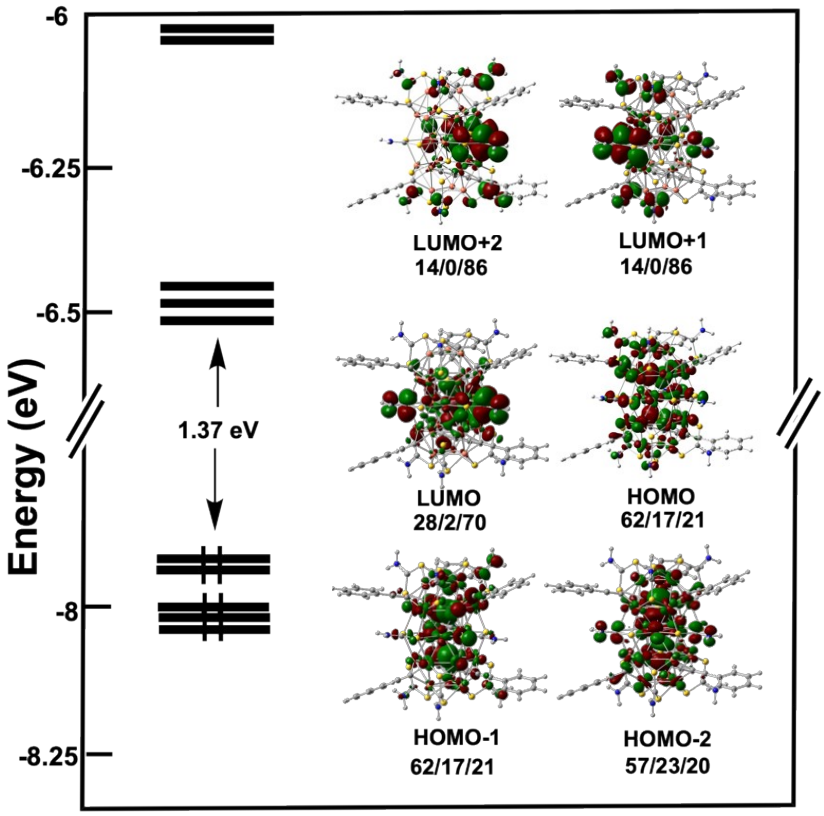

Figure S15. The Kohn-Sham MO diagram of $\mathbf{Cu_{21}S_2}$. The orbital localization (in %) is given in the order Cu/Sulfides/ligands.

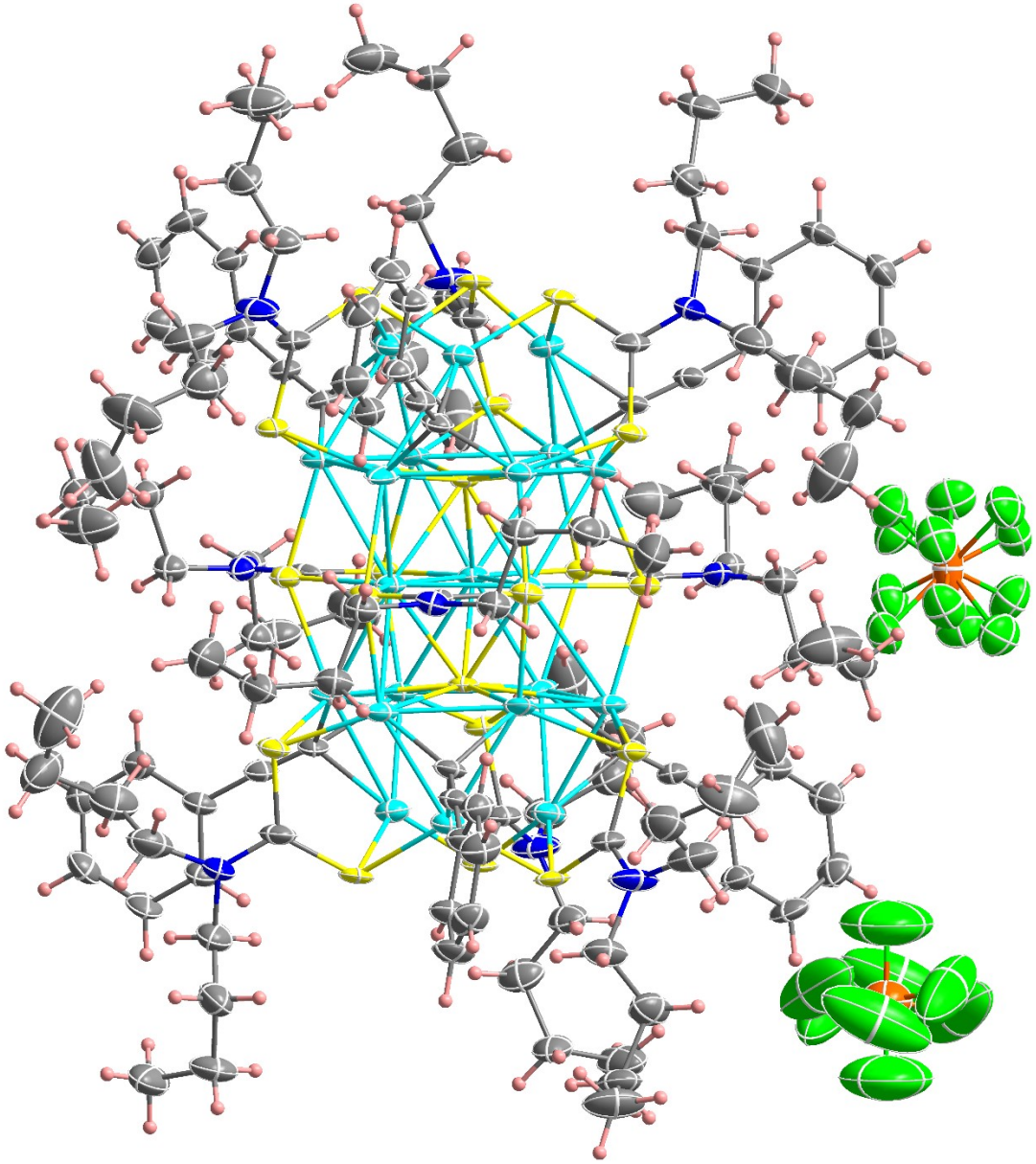

Figure S16. Thermal ellipsoid drawing (50%) of $[Cu_{21}S_2\{S_2CN^nBu_2\}_9(C_2Ph)_6](PF_6)_2$. Color code: Skin, H; gray, C; Blue, N; Yellow, S; Sky blue, Cu; orange, P; green, F.

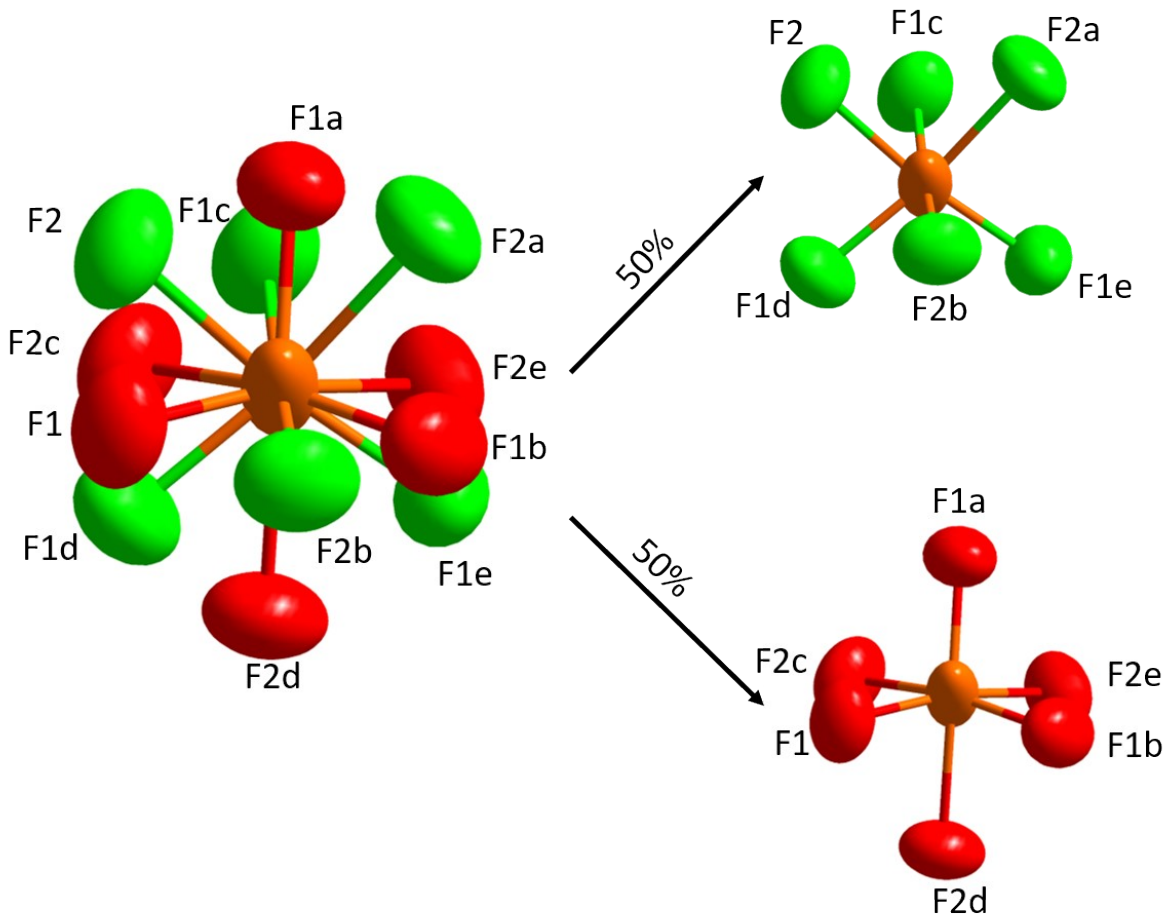

Figure S17. The disordered counter ion $[PF_6]^-$. Symmetry code: a, -x+y, 1-x, z; b, 1-y, 1+x-y, z; c, x, 1+x-y, 1.5-z; d, -x+y, y, 1.5-z; e, 1-y, 1-x, 1.5-z.

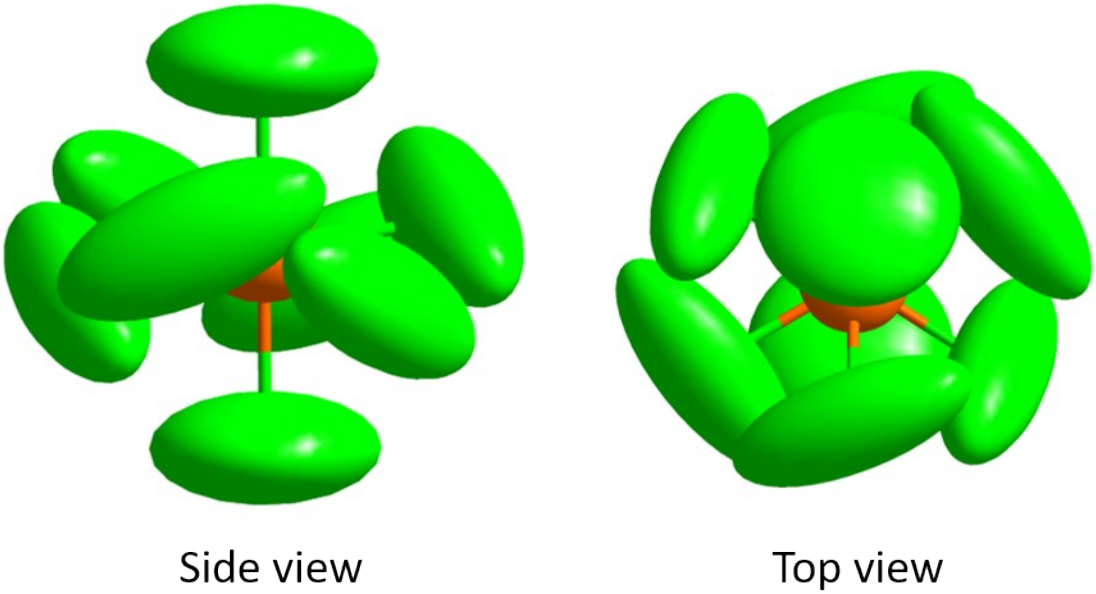

Figure S18. The second disordered counter-ion $[PF_6]^-$.

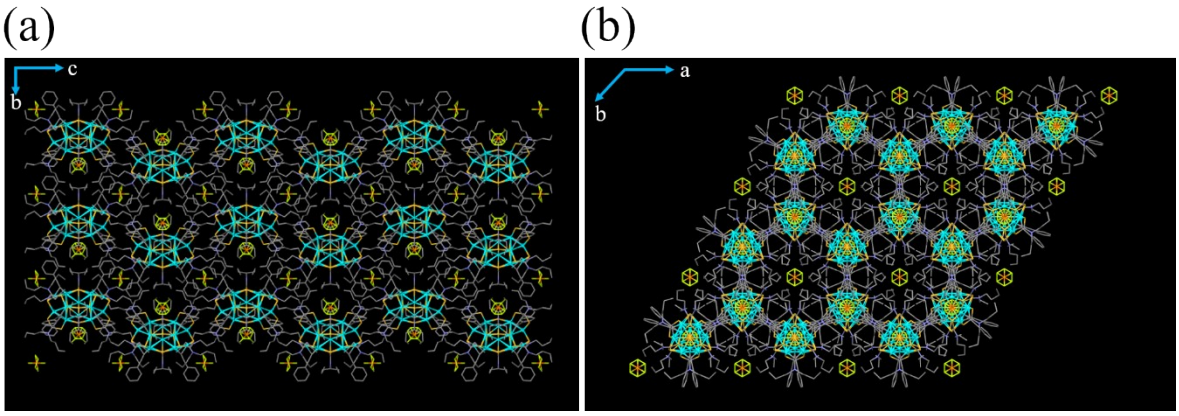

Figure S19. The packing diagram of $\mathbf{Cu_{21}S_2}$ viewed along (a) a-axis (b) c-axis.

a) $[Cu_{15}H_2\{S_2CN^nBu_2\}_6(C_2Ph)_6](PF_6)$ —(2.0 equiv. CF_3COOH, Acetone, RT, 10 mins)→ $[Cu_{21}S_2\{S_2CN^nBu_2\}_9(C_2Ph)_6](PF_6)_2$, yield 15 % based on Cu

$Cu_{15}H_2$ → **$Cu_{21}S_2$**

b) $[Cu_{12}S\{S_2CN^nBu_2\}_6(C_2Ph)_4] + NBu_4PF_6$ —(2.0 equiv. CF_3COOH, $CHCl_3$, RT, 10 mins)→ $[Cu_{21}S_2\{S_2CN^nBu_2\}_9(C_2Ph)_6](PF_6)_2$, yield 20 % based on Cu

$Cu_{12}S$ → **$Cu_{21}S_2$**

c) $11[Cu(CH_3CN)_4](PF_6) + 5[K\{S_2CN^nBu_2\}] + Na_2S_2O_3 + 3HC_2Ph$

(Et_3N, THF-CH_3CN, 50°C)

$[Cu_{21}S_2\{S_2CN^nBu_2\}_9(C_2Ph)_6](PF_6)_2$

yield 23 % based on Cu

$Cu_{21}S_2$

Scheme S1. Synthesis of **$Cu_{21}S_2$** from either acid treatment or one-pot synthesis method.

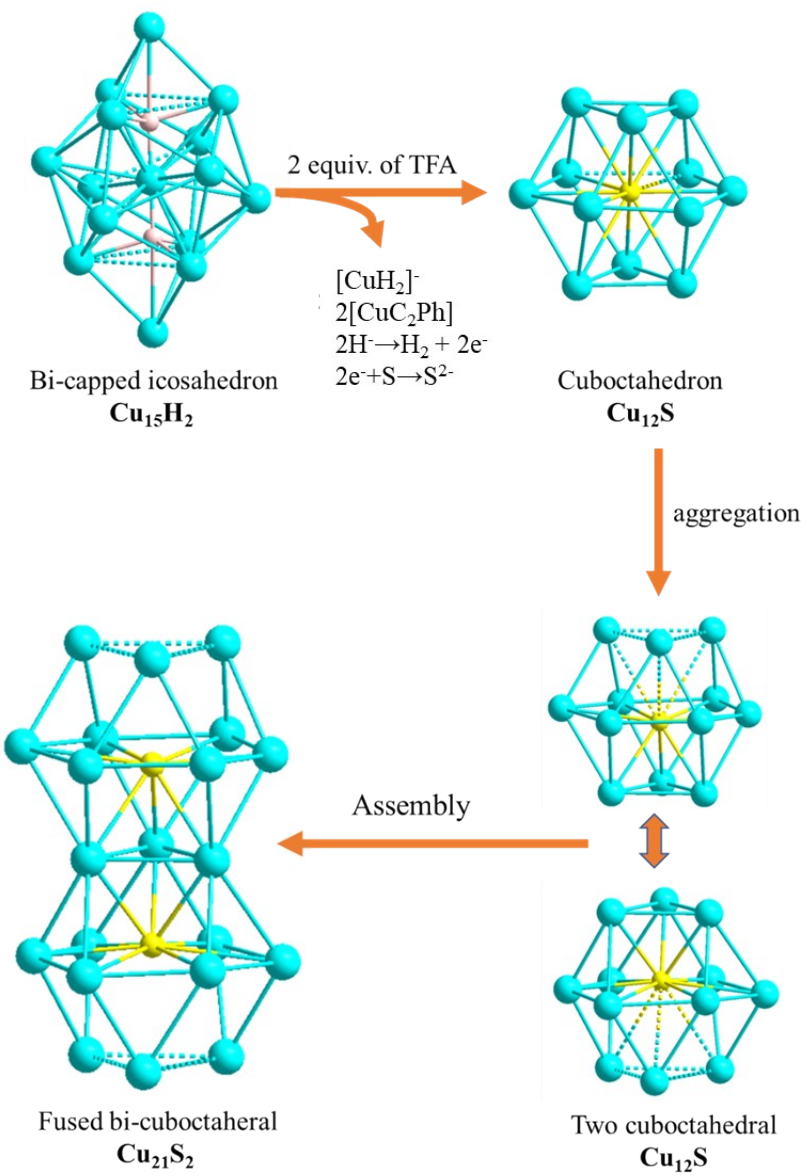

Scheme S2. The core structural change of bi-capped icosahedron $\mathbf{Cu_{15}H_2}$ into fused bi-cuboctahedral $\mathbf{Cu_{21}S_2}$. Color code: blue, Cu; yellow, S.

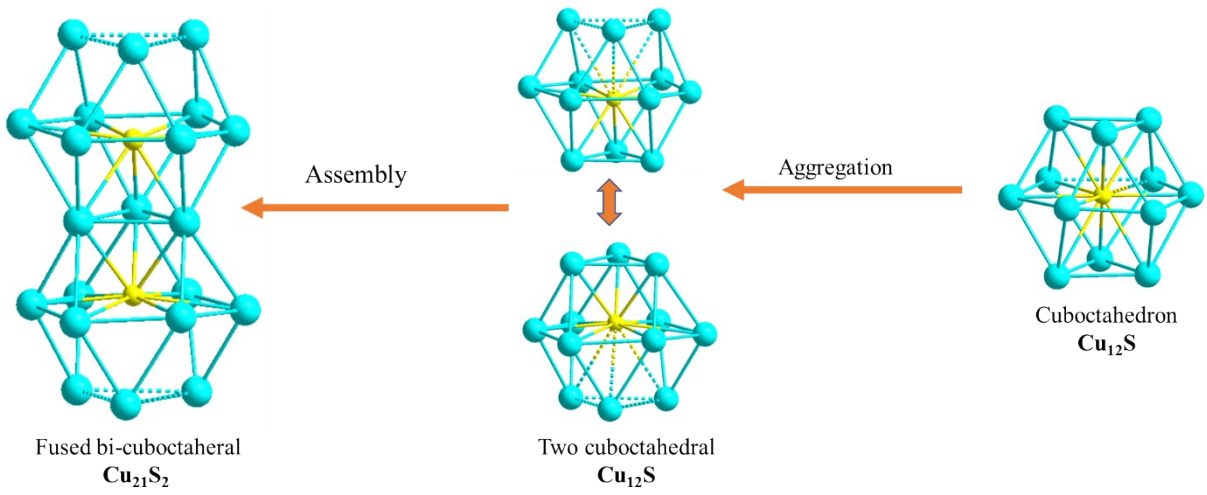

Scheme S3. The core structural change of sulfured-centred Cu_{12} cuboctahedron (**$Cu_{12}S$**) into fused bi-cuboctahedral **$Cu_{21}S_2$**. Color code: blue, Cu; yellow, S.

Table S1. Selected X-ray crystallographic data of $\mathbf{Cu_{21}S_2}$.

	$PdHCu_{11}$
CCDC no.	2269528
Empirical formula	$C_{129}H_{192}Cu_{21}F_{12}N_9P_2S_{20}$
Formula weight	4134.38
Temperature, K	100(2)
Wavelength, Å	0.71073
Crystal system	Trigonal
Space group	P-31*c*
a Å	17.3556(7)
b, Å	17.3556(7)
c, Å	29.8314(19)
α, deg.	90
β, deg.	90
γ, deg.	120
Volume, $Å^3$	7781.9(8)
Z	2
ρ, Mg m^{-3}	3.152
μ, mm^{-1}	4192
Crystal size, mm^3	0.180 x 0.120 x 0.100
θ_{max}, deg.	26.454
Reflections collected / unique	33121 / 5354 (R_{int} = 0.0628)
Completeness, %	100.0
restraints/parameters	6 / 308
GOF	1.021
[a]*R*1, [b]*wR*2 [I>2σ(I)]	*R*1 = 0.0641, *wR*2 = 0.1682
[a]*R*1, [b]*wR*2 (all data)	*R*1 = 0.0941, *wR*2 = 0.1939
Largest diff. peak/hole, e $Å^{-3}$	2.460, -1.040

[a] $R1 = \Sigma \big| \, | F_o | - | Fc | \, \big| / \Sigma | F_o |$.[b] $wR2 = \{\Sigma[w(F_o^2 - F_c^2)^2]/\Sigma[w(F_o^2)^2]\}^{1/2}$.

References

1. G. J. Kubas. *Inorg. Synth.,* 1979, **19**, 90-92.
2. G. Kaugars, and V. L. Rizzo. *J. Heterocycl. Chem*., 1981, **18**, 411-412.
3. K. K. Chakrahari, J. Liao, R. P. B. Silalahi, T.-H. Chiu, J.-H. Liao, X. Wang, S. Kahlal, J.-Y. Saillard, and C. W. Liu. *Small,* 2021, **17**, 2002544.
4. G. M. Sheldrick. SADABS, version 2014-11.0, Bruker Area Detector Absorption Corrections; Bruker AXS Inc.: Madison, WI, 2014.
5. G. M. Sheldrick. SAINT, v4.043, Software for the CCD Detector System; Siemens Analytical Instruments: Madison, WI, 1995.
6. G. M. Sheldrick. *Acta Crystallogr., Sect. A: Found. Crystallogr.,* 2008, **A64**, 112–122, DOI: 10.1107/S0108767307043930
7. T. Gruene, H. W. Hahn, A. V. Luebben, F. Meilleur, and G. M. Sheldrick. *J. Appl. Crystallogr.,* 2014, **47**, 462– 466, DOI: 10.1107/S1600576713027659
8. G. M. Sheldrick. SHELXL, version 6.14 (PC version) Program Library for Structure Solution and Molecular Graphics, Bruker Analytical X-ray Systems, Madison, Wisconsin, USA, 2003**.**
9. M. J. Frisch, G. W. Trucks, H. B. Schlegel, G. E. Scuseria, M. A. Robb, J. R. Cheeseman, G. Scalmani, V. Barone, G. A. Petersson, H. Nakatsuji, X. Li, M. Caricato, A. V. Marenich, J. Bloino, B. G. Janesko, R. Gomperts, B. Mennucci, H. P. Hratchian, J. V. Ortiz, A. F. Izmaylov, J. L. Sonnenberg, D. Williams-Young, F. Ding, F. Lipparini, F. Egidi, J. Goings, B. Peng, A. Petrone, T. Henderson, D. Ranasinghe, V. G. Zakrzewski, J. Gao, N. Rega, G. Zheng, W. Liang, M. Hada, M. Ehara, K. Toyota, R. Fukuda, J. Hasegawa, M. Ishida, T. Nakajima, Y. Honda, O. Kitao, H. Nakai, T. Vreven, K. Throssell, Jr. J. A. Montgomery, J. E. Peralta, F. Ogliaro, M. J. Bearpark, J. J. Heyd, E. N. Brothers, K. N. Kudin, V. N. Staroverov, T. A. Keith, R. Kobayashi, J. Normand, K. Raghavachari, A. P. Rendell, J. C. Burant, S. S. Iyengar, J. Tomasi, M. Cossi, J. M. Millam, M. Klene, C. Adamo, R. Cammi, J. W. Ochterski, R. L. Martin, K. Morokuma, O. Farkas, J. B. Foresman, and D. J. Fox. *Gaussian, Inc.*, Wallingford CT, 2016; Gaussian 16, Revision A.03.
10. F. Weigend, and R. Ahlrichs. *Phys. Chem. Chem. Phys*., 2005, **7**, 3297-3305.
11. A. D. Becke. *Phys. Rev. A.,* 1988, **38**, 3098-3100.
12. J. P. Perdew. *Phys. Rev. B.,* 1986, ***33***, 8822-8824.
13. A. E. Reed, and F. Weinhold. *J. Chem. Phys*., 1983, **78**, 4066-4073.
14. J. E. Carpenter, and F. Weinhold. *J. Mol. Struct. (Theochem).,* 1988, **169**, 41-62.

15. A. E. Reed, L. A. Curtiss, and F. Weinhold. *Chem. Rev*., 1988, **88**, 899-926.
16. T. Yanai, D. P. Tew, and N. C. Handy. *Chem. Phys. Lett*., 2004, **393**, 51-57.
17. S. I. Gorelsky. SWizard program, revision 4.5, http://www.sg-chem.net.